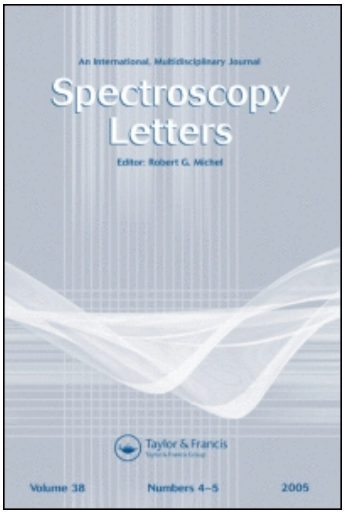

Spectroscopy Letters
Publication details, including instructions for authors and subscription information:
http://www.informaworld.com/smpp/title~content=t713597299

Comparative Study on Excitation Mechanism of Chromium Emission Lines in Argon Radio-Frequency Inductively-Coupled Plasma, Nitrogen Microwave Induced Plasma, and Argon or Nitrogen Glow Discharge Plasmas

Kazuaki Wagatsuma[a]; Yûetsu Danzaki[a]; Taketoshi Nakahara[b]
[a] The Institute for Materials Research, Tohoku University, Sendai, Japan [b] Department of Applied Chemistry, Graduate School of Engineering, Osaka Prefecture University, Osaka, Japan

Online publication date: 29 April 2003

To cite this Article Wagatsuma, Kazuaki , Danzaki, Yûetsu and Nakahara, Taketoshi(2003) 'Comparative Study on Excitation Mechanism of Chromium Emission Lines in Argon Radio-Frequency Inductively-Coupled Plasma, Nitrogen Microwave Induced Plasma, and Argon or Nitrogen Glow Discharge Plasmas', Spectroscopy Letters, 36: 1, 99 — 115
To link to this Article: DOI: 10.1081/SL-120021177
URL: http://dx.doi.org/10.1081/SL-120021177

SPECTROSCOPY LETTERS
Vol. 36, Nos. 1 & 2, pp. 99–115, 2003

Comparative Study on the Excitation Mechanism of Chromium Emission Lines in the Argon Radio-Frequency Inductively-Coupled Plasma, Nitrogen Microwave Induced Plasma, and Argon or Nitrogen Glow Discharge Plasmas

Kazuaki Wagatsuma,[1,*] Yûetsu Danzaki,[1] and Taketoshi Nakahara[2]

[1]The Institute for Materials Research, Tohoku University, Sendai, Japan
[2]Department of Applied Chemistry, Graduate School of Engineering, Osaka Prefecture University, Sakai, Osaka, Japan

ABSTRACT

Boltzmann plots of both atomic and ionic chromium emission lines are investigated to compare the excitation mechanisms in four different plasmas: an argon inductively-coupled plasma (Ar-ICP), a nitrogen high-power microwave induced plasma (N_2-MIP), an argon glow discharge plasma (Ar-GDP), and a nitrogen glow discharge plasma (N_2-GDP). The plots of the atomic lines and the ionic lines give both linear relationships

*Correspondence: Kazuaki Wagatsuma, The Institute for Materials Research, Tohoku University, Katahira 2-1-1, Sendai 980-8577, Japan; E-mail: kwagatsuma@mm.neweb.ne.jp.

DOI: 10.1081/SL-120021177
0038-7010 (Print); 1532-2289 (Online)

MARCEL DEKKER, INC.
270 Madison Avenue, New York, New York 10016

as well as similar excitation temperatures in the case of the Ar-ICP, the N_2-MIP, and the N_2-GDP. It implies that a thermodynamic process such as electron collision would control their excitations. However, only in the case of the ionic-line plot in the Ar-GDP, a departure from linear relationship is observed and the estimated excitation temperature is rather higher than that with the atomic lines, meaning that a specific excitation mechanism exists in the Ar-GDP. A possible explanation for these results is that a charge-transfer collision between chromium atom and argon ion plays a dominant role in exciting highly-lying energy levels of chromium ion, especially in the Ar-GDP.

Key Words: Boltzmann plot; Chromium; Argon glow discharge plasma; Argon inductively coupled plasma; Nitrogen glow discharge plasma; Nitrogen microwave induced plasma; Excitation mechanism; Charge-transfer collision.

INTRODUCTION

Various kinds of plasmas are now being employed in analytical emission spectrometry: for example, the argon inductively-coupled plasma (Ar-ICP) and the high-power nitrogen microwave induced plasma (N_2-MIP) for elemental analysis in aqueous solution, together with the low-power helium MIP as a detector of GC/LC, and spark discharge or argon glow discharge plasmas (Ar-GDP) for direct analysis of solid samples.[1,2] These plasmas have very different characteristics on the excitation as well as the sampling processes,[2] which determine each analytical application. Physical measurements, such as gas temperature and electron density, can provide useful information on the characteristics of the plasmas.[3,4] By means of the physical parameters, comparative studies among different plasmas enable the excitation mechanisms to be clarified, so that their discharge conditions can be optimized and that suitable analytical lines can be selected for analytical applications.

The use of a Boltzmann plot to measure the excitation temperature is extensively applied to obtain information about the excitation of emission, because it is not necessary to estimate the absolute emission intensity and to know the concentration of emitting species.[3] The Boltzmann distribution among different energy states exists in a plasma that is in local thermodynamic equilibrium (LTE);[3] however, analytical plasmas are not always in LTE.[5–13] This implies that the excitation temperature of such plasmas is not unique, but sometimes varies depending on the kind of emission lines employed. Therefore, it is important to determine whether a particular plasma is in LTE, and further to study why the plasma has non-LTE characteristics in the case where LTE is not established.

Marcel Dekker, Inc.
270 Madison Avenue, New York, New York 10016

In this paper, we present a comparison of the Boltzmann plots of chromium atomic and ionic lines when using an Ar-ICP, a N_2-MIP, an Ar-GDP, and a N_2-GDP as the excitation source. It was revealed from these plots that the excitation temperatures varied depending on the kind of the plasma and that some departures from a linear Boltzmann plot were observed especially in the Ar-GDP. In addition, we estimated the intensity ratio of Ar-GDP/Ar-ICP for various ionic lines of chromium, and a large variation in the intensity ratio was found when their excitation energies exceeded a certain value. The excitation mechanisms are discussed from these results.

EXPERIMENTAL

ICP and GDP Spectrometry

An ICP spectrometer system with a Czerny-Turner mounting monochromator (Hitachi model P-5200, Japan) was employed for measurements using an ICP or a GDP emission source. The ICP apparatus has already been reported elsewhere.[14] For the GDP measurement, the ICP torch was replaced with a Grimm-style glow discharge lamp. The ICP source comprised a three-turn load coil of 26 mm in inner diameter and a Fassel-type fused-silica torch having an 18-mm-diameter outer tube. The glow discharge lamp was made in-house according to the original model by Grimm.[15] The structure of the lamp has been described in our previous paper.[16] The inner diameter of the hollow anode was 8.0 mm and the gap between the electrodes was adjusted to be c.a. 0.3 mm.

A chromium plate (99.9%, purity) was prepared for the GDP measurement. It was polished with water proof emery paper and then rinsed with ethanol. Before measurements, a pre-discharge step was carried out for more than 10 min, to remove the surface contaminants. High-purity argon or nitrogen was employed as the plasma gas. A stock solution for the ICP measurement was prepared by dissolving 99.9-%-purity chromium metal, 1.000 g, with 200-m*l* hydrochloric acid (6 M) at room temperatures. The sample solution containing 1.0-mg/m*l* chromium was made by diluting the stock solution with de-ionized water. The solution contained ca. 1.4-M hydrochloric acid. Table 1(a) and (b) give the operating conditions for the GDP and the ICP in detail.

MIP Spectrometry

An ICP spectrometer system with a sequential monochromator (Nippon Jarrell-Ash model ICAP-575 II, Japan) was employed. The excitation

MARCEL DEKKER, INC.
270 Madison Avenue, New York, New York 10016

Table 1. Operating conditions for GDP (a), ICP (b), and MIP (c).

(a) GDP	
Plasma gas	Argon (99.9995%) or Nitrogen (99.9998%)
Gas pressure	530 Pa (4 Torr)
Discharge voltage	d.c. 350–800 V (constant voltage mode)
(b) ICP	
R.f. frequency	27.12 MHz
Forward power	1.0 kW
Reflected power	less than 20 W
Plasma gas	Argon (laboratory grade)
Gas flow	Outer 12 l/min
	Intermediate 0.50 l/min
	Carrier: 0.45 l/min
Observation height	15 mm above load coil
(c) MIP	
Driving frequency	2.45 GHz
Forward power	1.0 kW
Plasma gas	Nitrogen (laboratory grade)
Gas flow	Outer 15 l/min
	Carrier 0.6 l/min

source was replaced with an Okamoto cavity[17] and a magnetron power generator to generate an annular-shaped plasma with nitrogen gas. This apparatus has already been reported elsewhere.[18] The sample solution was the same as that used in the ICP spectrometry. Table 1(c) gives the operating conditions for the MIP.

RESULTS AND DISCUSSION

Analytical Lines

In selecting analytical emission lines for the Boltzmann plots, the following conditions should be satisfied: a large range in their excitation energy, accurate gA values, and line positions at closely spaced wavelengths to avoid a calibration of the wavelength dependence of the detector sensitivity. When considering these conditions, we employed two sets of chromium emission lines: 14 atomic lines (Cr I) at wavelengths between 373.08 and 389.40 nm and 13 ionic lines (Cr II) at wavelengths between 282.23 and 287.38 nm. The details are shown in Tables 2 and 3. The Cr I lines are classified into three groups: $3d^5(^6S)4p\ ^5P$-$3d^5(^6S)4s\ ^7S$,

Table 2. Atomic chromium lines for the Boltzmann plot.

Wavelength (nm)	Upper level	(eV)	Lower level	(eV)	gA-value $\times 10^8$
373.081	$3d^5(^6\mathbf{S})4p\ ^5\mathbf{P}_2$	3.3222	$3d^5(^6\mathbf{S})4s\ ^7\mathbf{S}_3$	0.0000	0.011
373.203	$3d^5(^6\mathbf{S})4p\ ^5\mathbf{P}_3$	3.3212	$3d^5(^6\mathbf{S})4s\ ^7\mathbf{S}_3$	0.0000	0.008
374.389	$3d^4(^3\mathbf{H})4s4p(^3\mathbf{P})\ ^5\mathbf{G}_6$	5.8547	$3d^5(^4\mathbf{G})4s\ ^5\mathbf{G}_6$	2.5440	9.893
374.449	$3d^4(^3\mathbf{H})4s4p(^3\mathbf{P})\ ^5\mathbf{G}_6$	5.8547	$3d^5(^4\mathbf{G})4s\ ^5\mathbf{G}_5$	2.5446	0.651
375.717	$3d^4(^3\mathbf{H})4s4p(^3\mathbf{P})\ ^5\mathbf{G}_3$	5.8427	$3d^5(^4\mathbf{G})4s\ ^5\mathbf{G}_2$	2.5438	0.431
375.766	$3d^4(^3\mathbf{H})4s4p(^3\mathbf{P})\ ^5\mathbf{G}_3$	5.8427	$3d^5(^4\mathbf{G})4s\ ^5\mathbf{G}_3$	2.5442	2.891
375.804	$3d^4(^3\mathbf{H})4s4p(^3\mathbf{P})\ ^5\mathbf{G}_3$	5.8427	$3d^5(^4\mathbf{G})4s\ ^5\mathbf{G}_4$	2.5446	0.812
376.824	$3d^4(^3\mathbf{H})4s4p(^3\mathbf{P})\ ^5\mathbf{G}_2$	5.8330	$3d^5(^4\mathbf{G})4s\ ^5\mathbf{G}_2$	2.5438	2.550
376.873	$3d^4(^3\mathbf{H})4s4p(^3\mathbf{P})\ ^5\mathbf{G}_2$	5.8330	$3d^5(^4\mathbf{G})4s\ ^5\mathbf{G}_3$	2.5442	0.595
388.329	$3d^4(^5\mathbf{D})4s4p(^3\mathbf{P})\ ^5\mathbf{D}_3$	4.1746	$3d^44s^2\ ^5\mathbf{D}_2$	0.9829	0.273
388.522	$3d^4(^5\mathbf{D})4s4p(^3\mathbf{P})\ ^5\mathbf{D}_2$	4.1586	$3d^44s^2\ ^5\mathbf{D}_1$	0.9684	0.195
388.680	$3d^4(^5\mathbf{D})4s4p(^3\mathbf{P})\ ^5\mathbf{D}_4$	4.1926	$3d^44s^2\ ^5\mathbf{D}_3$	1.0037	0.198
389.404	$3d^4(^5\mathbf{D})4s4p(^3\mathbf{P})\ ^5\mathbf{D}_1$	4.1439	$3d^44s^2\ ^5\mathbf{D}_0$	0.9610	0.117
390.291	$3d^4(^5\mathbf{D})4s4p(^3\mathbf{P})\ ^5\mathbf{D}_2$	4.1586	$3d^44s^2\ ^5\mathbf{D}_2$	0.9829	0.175

$3d^4(^5D)4s4p\ ^5D$-$3d^44s^2\ ^5D$, and $3d^4(^3H)4s4p(^3P)\ ^5G$-$3d^5(^4G)4s\ ^5G$ transitions.[19] Their excitation energies range from 3.32 to 5.85 eV, and all the corresponding gA values were published by Wiese et al.,[20] as shown in the sixth column of Table 2. In general, attention should be put on the self-absorption effect when estimating the emission intensities of

Table 3. Ionic chromium lines for the Boltzmann plot.

Wavelength (nm)	Upper level	(eV)	Lower level	(eV)	gA-value $\times 10^8$
282.238	$3d^4(^3\mathbf{H})4p\ ^4\mathbf{I}_{15/2}$	8.1595	$3d^4(^3\mathbf{H})4s\ ^4\mathbf{H}_{13/2}$	3.7680	36.8
284.001	$3d^4(^3\mathbf{H})4p\ ^4\mathbf{I}_{11/2}$	8.1108	$3d^4(^3\mathbf{H})4s\ ^4\mathbf{H}_{9/2}$	3.7466	32.4
284.983	$3d^4(^5\mathbf{D})4p\ ^6\mathbf{F}_{7/2}$	5.8553	$3d^4(^5\mathbf{D})4s\ ^6\mathbf{D}_{5/2}$	1.5061	7.36
285.134	$3d^4(^3\mathbf{H})4p\ ^4\mathbf{I}_{9/2}$	8.0858	$3d^4(^3\mathbf{H})4s\ ^4\mathbf{H}_{7/2}$	3.7389	22.0
285.677	$3d^4(^5\mathbf{D})4p\ ^4\mathbf{D}_{5/2}$	6.7726	$3d^4(^5\mathbf{D})4s\ ^4\mathbf{D}_{3/2}$	2.4339	2.58
285.740	$3d^4(^5\mathbf{D})4p\ ^4\mathbf{D}_{7/2}$	6.7923	$3d^4(^5\mathbf{D})4s\ ^4\mathbf{D}_{5/2}$	2.4546	2.24
286.092	$3d^4(^5\mathbf{D})4p\ ^6\mathbf{F}_{3/2}$	5.8154	$3d^4(^5\mathbf{D})4s\ ^6\mathbf{D}_{1/2}$	1.4830	2.76
286.258	$3d^4(^5\mathbf{D})4p\ ^6\mathbf{F}_{7/2}$	5.8553	$3d^4(^5\mathbf{D})4s\ ^6\mathbf{D}_{7/2}$	1.5255	5.04
286.672	$3d^4(^5\mathbf{D})4p\ ^6\mathbf{F}_{3/2}$	5.8154	$3d^4(^5\mathbf{D})4s\ ^6\mathbf{D}_{3/2}$	1.4918	4.80
286.709	$3d^4(^5\mathbf{D})4p\ ^4\mathbf{D}_{3/2}$	6.7569	$3d^4(^5\mathbf{D})4s\ ^4\mathbf{D}_{3/2}$	2.4339	4.40
286.764	$3d^4(^5\mathbf{D})4p\ ^6\mathbf{F}_{1/2}$	5.8052	$3d^4(^5\mathbf{D})4s\ ^6\mathbf{D}_{1/2}$	1.4830	2.20
287.043	$3d^4(^5\mathbf{D})4p\ ^4\mathbf{D}_{5/2}$	6.7726	$3d^4(^5\mathbf{D})4s\ ^4\mathbf{D}_{5/2}$	2.4546	7.80
287.381	$3d^4(^5\mathbf{D})4p\ ^4\mathbf{D}_{1/2}$	6.7468	$3d^4(^5\mathbf{D})4s\ ^4\mathbf{D}_{3/2}$	2.4339	1.76

atomic resonance lines. In the set of the Cr I lines, only two resonance lines that have fairly small transition probabilities, the 373.081-nm and the 373.203-nm lines, were included to prevent self-absorption. On the other hand, the Cr II lines are classified into three groups: $3d^4(^5D)4p\ ^6F\text{-}3d^4(^5D)4s\ ^6D$, $3d^4(^5D)4p\ ^4D\text{-}3d^4(^5D)4s\ ^4D$, and $3d^4(^3H)4p\ ^4I\text{-}3d^4(^3H)4s\ ^4H$ transitions.[19] Their excitation energies range from 5.80 to 8.15 eV, and all the corresponding gA values have also been published by Wiese et al.,[20] as shown in the sixth column of Table 3.

Boltzmann Plots

Figure 1 shows Boltzmann plots of the Cr I lines (a) as well as the Cr II lines (b) when an Ar-ICP is operated at an rf forward power of 1.0 kW. The emission intensities could be estimated with a good precision (the relative standard deviations ranged from 0.5 to 2%); therefore, each error bar is in most cases included in the symbol used to mark the experimental data points in the Figure. Both of the plots almost follow a linear relationship, meaning that LTE conditions are fulfilled in the Ar-ICP. Although some variance between the two resonance lines belonging to the 3.3-eV group is observed, a good linear relationship is fulfilled (the correlation coefficient for linear regression is calculated to be -0.9981). Because the variance always appears to be similar in all cases, it probably resulted from an uncertainty in the gA values; the gA values are likely to include some errors because these values are very small. These plots imply that a dominant thermal process controls the population among the energy levels, which have a wide range of excitation energies.

The results in an Ar-GDP are shown in Figure 2. One should notice that the Boltzmann plot of the Cr II lines (Figure 2b) is bent downwards, because the emission lines that originate from the 8.2-eV upper levels have larger intensities than the values expected from a straight line joining the other two groups of data, whereas the plot of the Cr I lines (Figure 2a) is a straight line as in the case of the Ar-ICP. Furthermore, Figure 3 shows that, in the N_2-GDP, the Boltzmann plot of the Cr II lines follows a linear relationship, which is different from the data of the Ar-GDP. These results imply that there is a particular excitation mechanism that is effective only for the high-lying energy levels, and only in the Ar-GDP. Table 4 indicates excitation temperatures estimated from the data of the Cr I lines and Cr II lines when four different plasmas are operated under each optimized discharge condition. Except for the Ar-GDP, little difference in the excitation temperatures is found. It seems that the Ar-ICP, the N_2-MIP, and the N_2-GDP are almost in LTE conditions. However, in the Ar-GDP, the excitation temperature estimated from the Cr II lines is twice as high as that

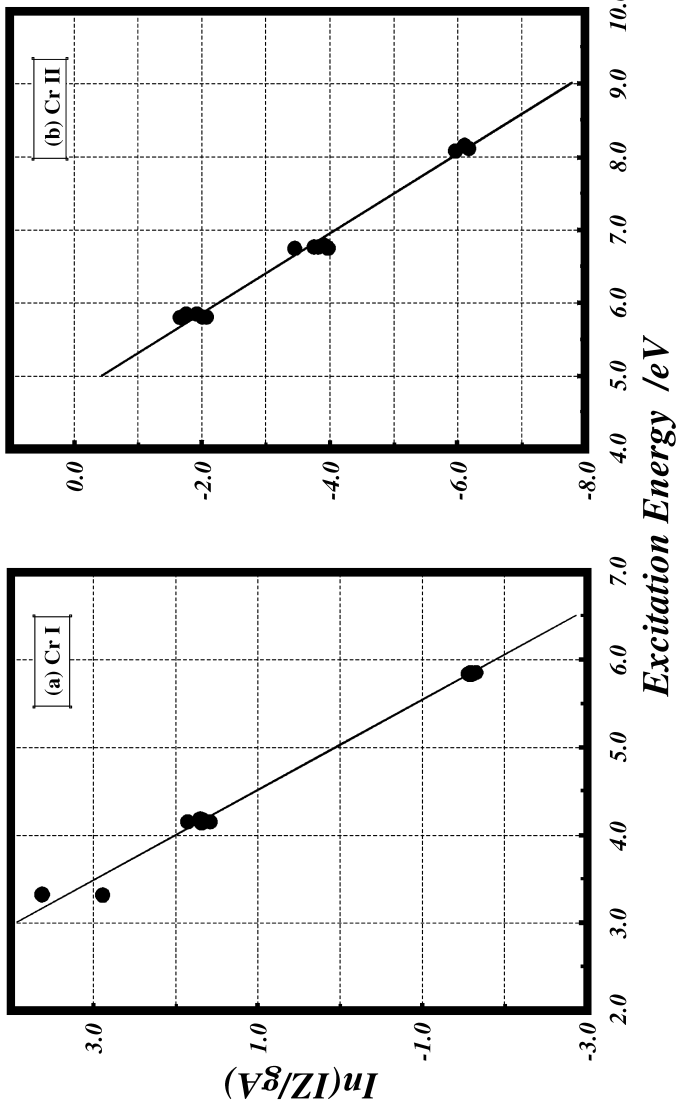

Figure 1. Boltzmann plots of Cr I lines (a) and Cr II lines (b) excited in Ar-ICP at the forward power of 1.0 kW. Plasma gases: 12 l/min (outer), 0.5 l/min (intermediate), and 0.5 l/min (carrier). Observation height: 15 mm; sample 1.0 mg/ml Cr in 1.4 M HCl solution.

MARCEL DEKKER, INC.
270 Madison Avenue, New York, New York 10016

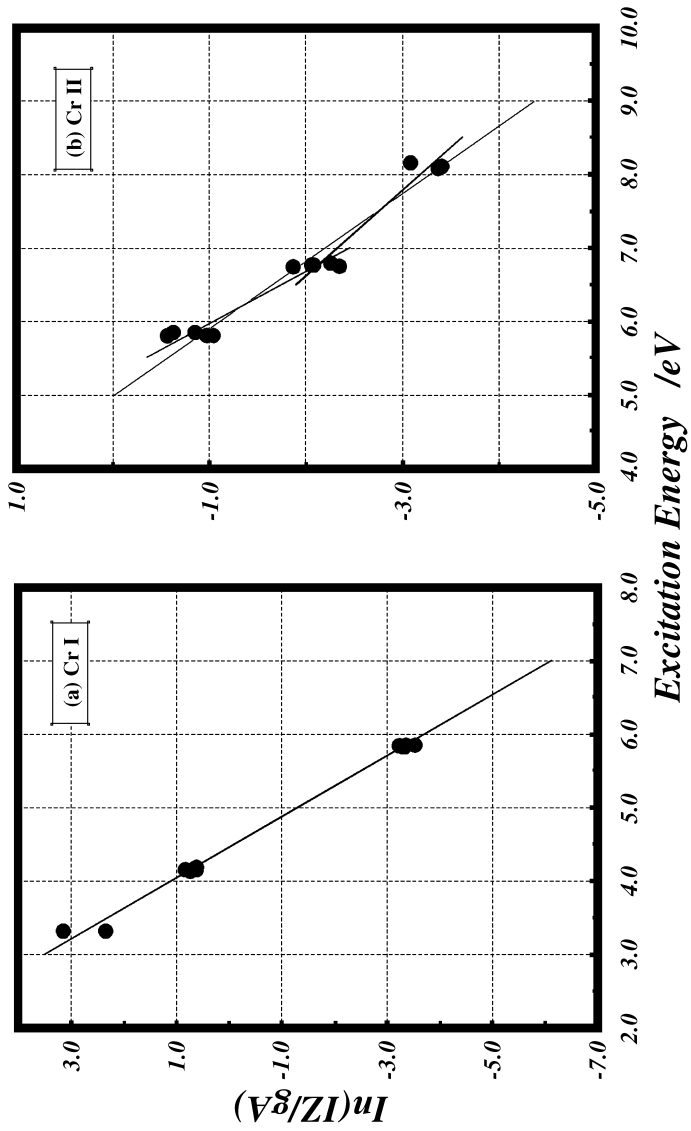

Figure 2. Boltzmann plots of Cr I lines (a) and Cr II lines (b) excited in Ar-GDP at the discharge power of 600 V/64 mA. Plasma gas: Ar 530 Pa; sample: Cr plate (99.9%).

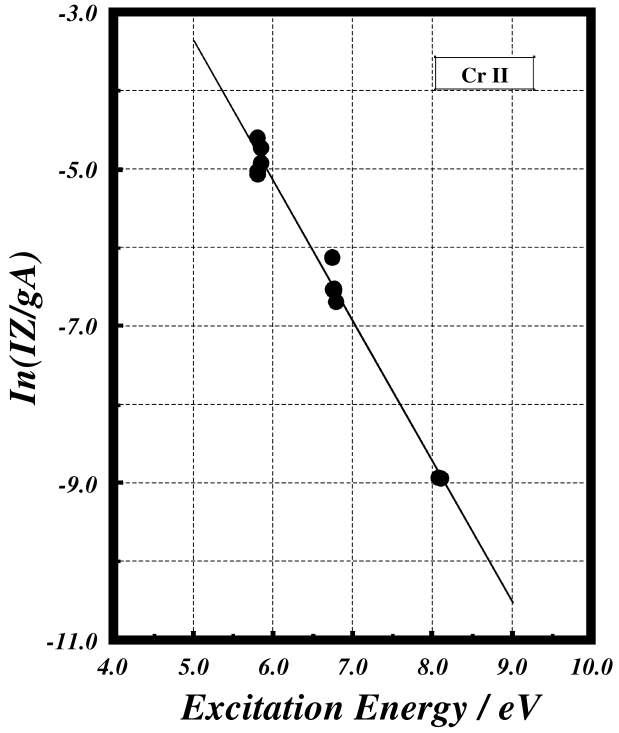

Figure 3. Boltzmann plots of Cr II lines emitted from N_2-GDP at the discharge power of 800 V/35 mA. Plasma gas: N_2 530 Pa; sample: Cr plate (99.9%).

from the Cr I lines, implying different major excitation mechanisms between the Cr I and the Cr II excited levels. Figure 4 shows variations in the excitation temperature calculated from the Cr I lines, as well as the Cr II lines, when the discharge voltage varies from 350 to 700 V in the Ar-GDP. Both of these excitation temperatures are almost constant independent

Table 4. Comparison in the excitation temperature estimated from Cr I and Cr II emission lines.

Temperature (K)	Ar-ICP	Ar-GDP	N2-GDP	N2-MIP
Cr I	6000	4900	6200	6300
Cr II	6300	11000	6300	5800
Conditions	1.0 kW	600 V	800 V	1.0 kW

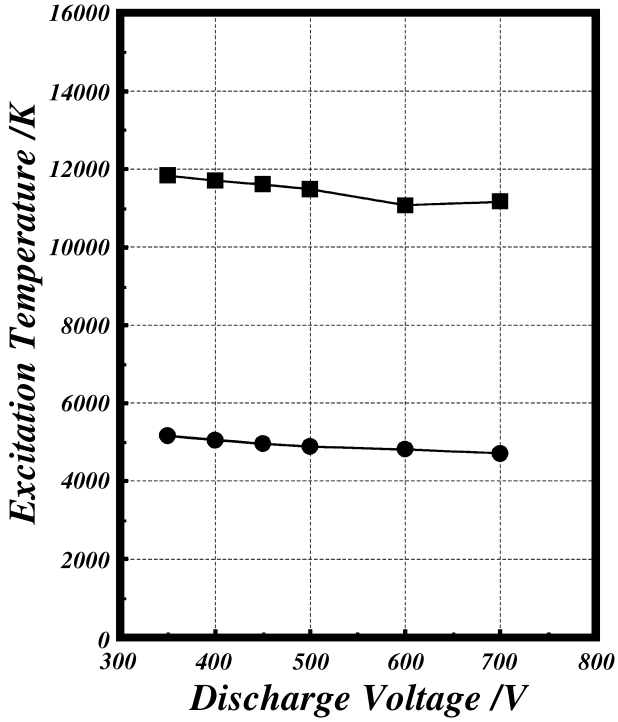

Figure 4. Excitation temperatures estimated from the Boltzmann plot of Cr I lines (circle) and Cr II lines (square) as a function of the discharge voltage in Ar-GDP. Plasma gas: Ar 530 Pa; sample: Cr plate (99.9%).

of the discharge voltage supplied. The kinetic energy of electrons emitted from the cathode should increase with increasing supplied voltages. It is thus likely to say that collisions with these energetic electrons hardly take part in the excitation of the chromium species, probably because their kinetic energies are too large for atomic chromium to be excited effectively. The collisions with electrons which are produced secondarily in the negative glow region can act as an alternative excitation channel for the chromium species, because such electrons occupy a larger part of the overall electrons and the kinetic energies are relatively small.[21] It is known that most of the potential drop exists, not in the negative glow, but in the cathode sheath;[21] therefore, the energy of the secondary electrons would be less affected by the applied discharge voltage and thus the excitation temperatures are almost constant. As shown in Figure 4, a large

temperature difference between the Cr I and the Cr II lines is always observed over a wide range of the discharge voltage. We thus consider that some non-thermodynamic excitation processes are concerned with the excitation of the Cr II lines.

The chromium spectrum comprises a number of Cr II lines of which excitation energies widely vary from 6 to 11 eV.[22] Unfortunately, most of the Cr II lines, which have an excitation energy of 8 to 11 eV, cannot be employed for estimation of the excitation temperature, because the corresponding gA values are lacking in the literature.[20,23] However, the intensities of these Cr II lines would provide interesting knowledge about the excitation mechanism. It is not possible to compare the data of the Ar-GDP with those of the Ar-ICP directly, because of different amounts of chromium introduced into the plasmas as well as different discharge powers supplied to the plasmas. However, the intensity ratios are meaningful if they are compared with each other. Figure 5 shows a variation in the intensity ratio (Ar-GDP/Ar-ICP) for 56 Cr II lines between 251.8 and 287.7 nm, of which excitation energies vary from 5.81 to 10.91eV, as a function of the excitation energy. It should be noted that the intensity ratios for emission lines which have an excitation energy of more than 8 eV, are much larger compared to emission lines having lower excitation energies. The ratio is suddenly elevated at excitation energies of 8–9 eV, probably due to a selective excitation being much more effective for the high-lying energy levels in the Ar-GDP. The threshold value gives a key to a consideration of the excitation mechanism.

Mechanism

A possible reason for non-LTE behavior is that the excitation processes include non-thermodynamic collisions such as Penning ionization and charge-transfer collision.[24] A typical example is selective excitation/ionization that results from resonance charge-transfer collisions.[25] This causes a non-Boltzmann distribution among particular energy states to yield a non-linear Boltzmann plot. Several researchers have found that particular ionic lines of several elements are enhanced through charge-transfer collisions not only in GDP[9–13] but also in the Ar-ICP,[5–8] where the population of the corresponding energy levels is elevated due to good matching in the internal energies.[25] Mermet et al. have indicated that, in an Ar-ICP, the intensities of ionic lines which have a total energy of about 16 eV cannot be explained by temperature variations due to charge-transfer from argon ions.[26] Furthermore, Wagatsuma et al. have revealed, after analyzing the line intensity of singly-ionized vanadium, that a charge-transfer effect appears in the Ar-GDP more dominantly than in the Ar-ICP.[27]

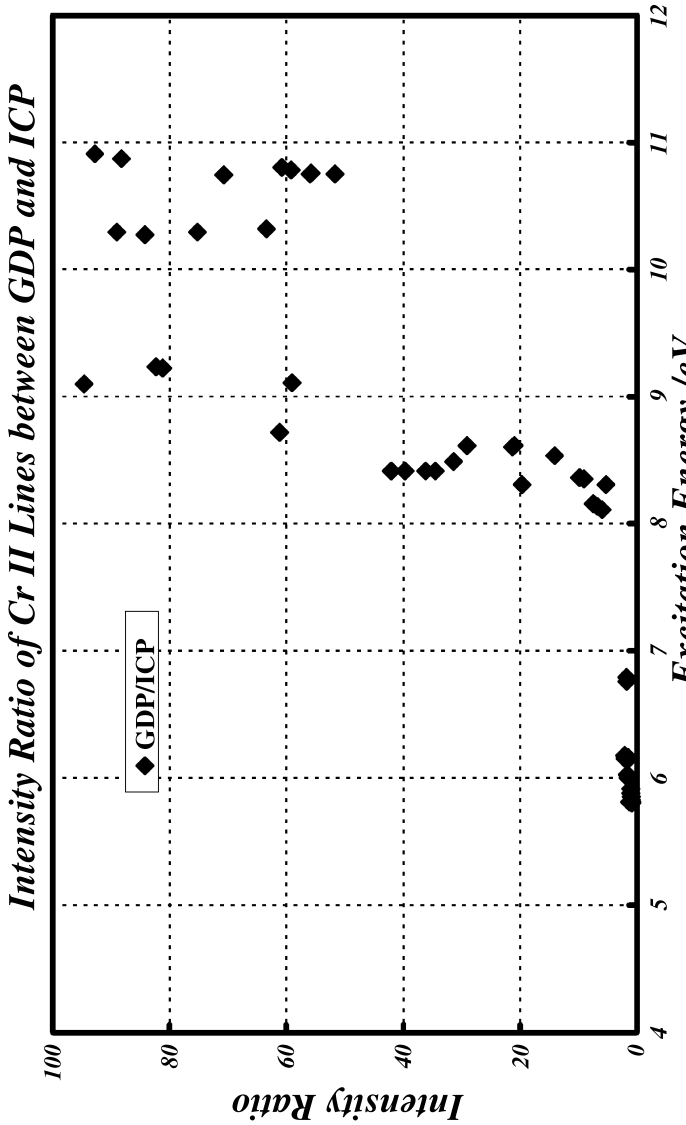

Figure 5. Variations in the intensity ratio of Cr II lines (Ar-GDP/Ar-ICP) as a function of the excitation energy.

Figure 6 shows a simplified energy diagram of the chromium ion, together with the ionic ground state of argon. In order to consider energy-transfer collisions occurring in the plasma, it is convenient to use values of the total energy, ionization and excitation; i.e., a scale whose origin is the level of the atomic ground state coinciding with that of the argon atom. The

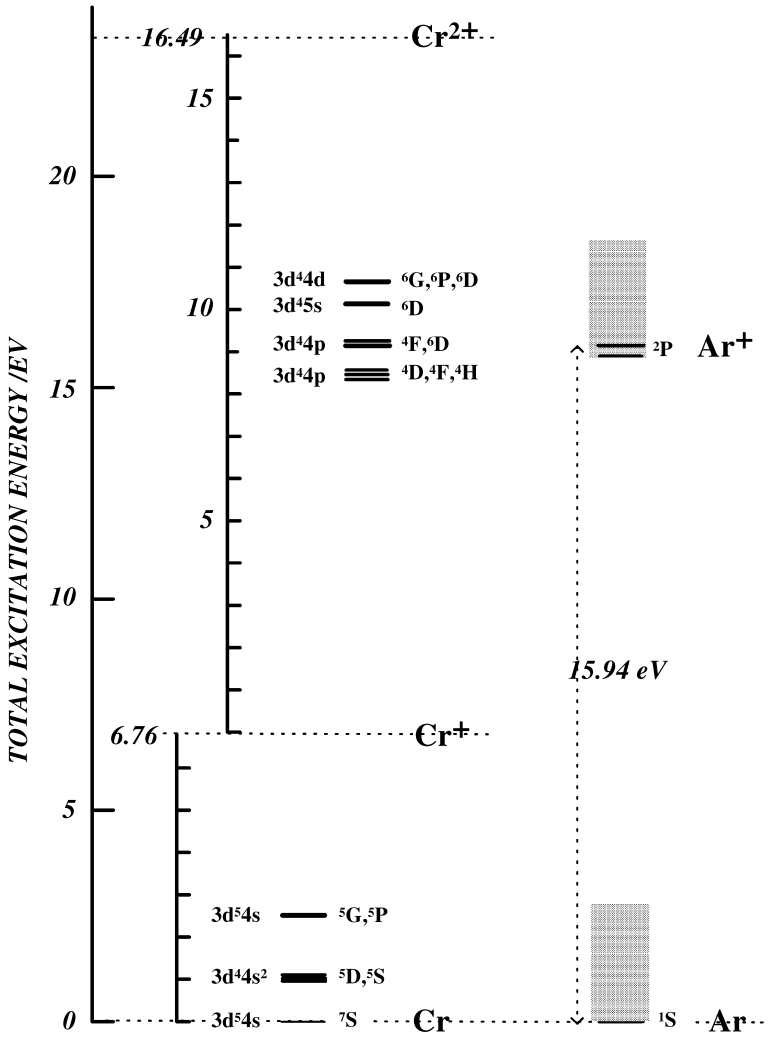

Figure 6. Schematic energy level diagram of chromium, together with the ionic ground state of argon.

MARCEL DEKKER, INC.
270 Madison Avenue, New York, New York 10016

total excitation energy is defined as the sum of the first ionization energy (6.76 eV)[19] and an excitation energy of ionic chromium. It should be noted that the total excitation energy of the $3d^4(^3D)4p\ ^4D$ levels is almost the same as that of the argon ion ground state ($3p^5\ ^2P_{1/2}$, 15.94 eV). From a good match in their total excitation energies, we can consider the following charge-transfer collision, for instance, for the Cr II 262.727-nm line:

$$\begin{aligned} &\mathrm{Cr}(3d^5(^6S)4s\ ^7S_3, 0.00\ \mathrm{eV}) + \mathrm{Ar}^+(3p^5\ ^2P_{1/2}, 15.94\ \mathrm{eV}) \\ &\quad \rightarrow \mathrm{Cr}^+\ \{3d^4(^3D)4p\ ^4D_{1/2}, (9.10 + 6.76)\ \mathrm{eV}\} \\ &\qquad + \mathrm{Ar}(3p^6\ ^1S_{1/2}, 0.00\ \mathrm{eV}) + \mathrm{D\ E}\ (0.08\ \mathrm{eV}) \end{aligned}$$

where the resulting excited state of Cr^+ has an internal energy corresponding to the sum of the first ionization potential and the excitation energy. The small difference in the total energies could contribute to resonance energy transfer,[25] thus leading to the increased population of the $3d^4(^3D)4p\ ^4D_{1/2}$ excited level. Whereas the intensity ratios (GDP/ICP) are almost unity in the emission lines which have an excitation energy of about 6 eV, those of the emission lines which have an excitation energy of about 9 eV become much larger. This indicates that charge-transfer collisions work much more dominantly in the Ar-GDP, probably due to longer lifetime of argon ions, as the GDP is operated at reduced pressures. Figure 6 also shows that the intensity ratios are still larger even when the excitation energy ranges from 10 to 11 eV. It is insufficient to excite the energy levels having an energy of 10–11 eV through the charge-transfer collision in which argon ion in the ground state is involved. However, as shown in Figure 6, the ground state of atomic chromium consists of several energy levels ($3d^5(^6S)4s$, $3d^44s^2$, $3d^5(^4G)4s$, and $3d^5(^4P)4s$) whose excitation energies range from 0 to 2.7 eV.[19] Therefore, it is to be expected that these energy levels become an initial state of atomic chromium when the charge transfer collision occurs with argon ion. Furthermore, this mechanism would explain the non-linear Boltzmann plot as shown in Figure 2 and the difference in the excitation temperature as indicated in Table 3, because the intensities of the 282.238-nm and the 284.001-nm lines would be enhanced largely through the charge-transfer collision in the Ar-GDP rather than the Ar-ICP.

CONCLUSIONS

Different excitation temperatures between Cr I and Cr II lines are found, especially in the Ar-GDP, whereas the excitation temperatures are

similar in the Ar-ICP, the N_2-MIP, and the N_2-GDP. Also, an intensity enhancement of particular ionic lines is found in the Ar-GDP. It is considered that the major reason is the selective ionization/excitation through charge-transfer collision with argon ion, thus leading to the non-Boltzmann distribution among excited energy levels of chromium ion. The studies using Boltzmann plots provide useful knowledge on excitation mechanisms in such analytical emission sources.

ACKNOWLEDGMENT

A part of this work was carried out under the Visiting Researcher's Program of the Institute for Materials Research, Tohoku University, Japan. This study was in part supported by a grant-in-aid from the Ministry of Education of Japan (No. 09640713).

REFERENCES

1. Broekaert, J.A.C. *Atomic Emission Spectrometry. Analytical Atomic Spectrometry with Flames and Plasmas*; Wiley-VCH: Weinheim, 2002, 192–253.
2. Boumans, P.W.J.M. *Introduction to Atomic Emission Spectrometry. Inductively Coupled Plasma Emission Spectroscopy, Part 1*; John Wily & Sons: New York, 1987; 1–44.
3. Mermet, J.M. Spectroscopic diagnostics: basic concepts. In *Inductively Coupled Plasma Emission Spectroscopy, Part 2*; Boumans, P.W.J.M., Ed.; John Wily & Sons: New York, 1987; 353–386.
4. Griem, H.R. *Temperature Measurements. Plasma Spectroscopy*; McGraw-Hill: New York, 1964; 267–296.
5. Marichy, M.; Mermet, M.; Mermet, J.M. Relationship between detection limits and mechanisms in inductively coupled plasma atomic emission spectrometry. J. Anal. At. Spectrom. **1987**, *2*, 561–565.
6. Bricker, T.M.; Smith, F.G.; Houk, R.S. Charge transfer reactions between xenon ions and iron atoms in an argon-xenon inductively coupled plasma. Spectrochim. Acta **1995**, *50B*, 1325–1336.
7. Vicek, J. Magnesium as a representative analyte metal in argon inductively coupled plasma I. Spectrochim. Acta **1997**, *52B*, 599–606.
8. Ogilvie, C.M.; Fansworth, P.B. Correlation spectrometry as a probe of excitation and ionization mechanisms in the inductively coupled plasma. Spectrochim. Acta **1992**, *47B*, 1389–1402.

MARCEL DEKKER, INC.
270 Madison Avenue, New York, New York 10016

9. Steers, E.B.M.; Fielding, R.J. Charge-transfer excitation processes in the Grimm lamp. J. Anal. At. Spectrom. **1987**, *2*, 239–244.
10. Wagatsuma, K.; Hirokawa, K. Observations of bismuth and lead ionic emission lines excited from Grimm-type glow discharge plasmas with pure neon and neon-argon mixtures. J. Anal. At. Spectrom. **1989**, *4*, 525–528.
11. Wagatsuma, K.; Hirokawa, K. Spectrometric studies of excitation mechanisms on singly-ionized copper emission lines in Grimm-type glow discharge plasmas with helium mixture techniques. Spectrochim. Acta **1991**, *46B*, 269–281.
12. Steers, E.B.M.; Leis, F. Excitation of the spectra of neutral and singly ionized atoms in the Grimm-type discharge lamp, with and without supplementary microwave plasma. Spectrochim. Acta **1991**, *46B*, 527–537.
13. Wagatsuma, K.; Hirokawa, K. Classification of singly-ionized iron emission lines in 160–250 nm wavelength region from Grimm-type glow discharge plasma and the excitation mechanisms. Spectrochim. Acta **1996**, *51B*, 349–374.
14. Danzaki, Y.; Takada, K.; Wagatsuma, K.; Oku, M. Accurate and rapid estimation on spectral interference in routine analysis by ICP-AES: use of mutual interference coefficients. Fresenius' J. Anal. Chem. **1998**, *361*, 410–418.
15. Grimm, W. Eine Neue Glimmentladungslampe für die Optishe Emissionsspektral analyse. Spectrochim. Acta **1968**, *23B*, 443–454.
16. Wagatsuma, K.; Hirokawa, K. Observation of Cu-Ni alloy surfaces by low wattage glow discharge spectrometry. Surf. Interface Anal. **1984**, *6*, 167–170.
17. Okamoto, Y. Annular-shaped microwave-induced nitrogen plasma at atmospheric pressure for emission spectrometry of solutions. Anal. Sci. **1991**, *7*, 283–288.
18. Nakahara, T.; Li, Y. Determination of trace amounts of antimony in pure copper by high-power nitrogen microwave-induced plasma atomic emission spectrometry with hydride generation. J. Anal. At. Spectrom. **1998**, *13*, 401–405.
19. Moore, C.E. *Atomic Energy Levels*; NBS Circular 467: Washington, DC, 1952; Vol. 2, 1–13.
20. Martin, G.A.; Fuhr, J.R.; Wiese, W.L. Atomic transition probabilities scandium through manganese. J. Phys. Chem. Ref. Data **1988**, *17* (Suppl. No. 3), 311–342.
21. Chapman, B. *DC Glow Discharges. Glow Discharge Processes*; John Wily & Sons: New York, 1980; 77–138.
22. Wagatsuma, K. Wavelength table of chromium emission lines in argon

Marcel Dekker, Inc.
270 Madison Avenue, New York, New York 10016

glow discharge optical emission spectrometry. Fresenius' J. Anal. Chem. **2000**, *367*, 414–415.
23. Corliss, C.H.; Bozman, W.R. *Experimental Transition Probabilities for Spectral Lines of Seventy Elements*; NBS Monograph 53: Washington, DC, 1962.
24. Blades, M.W. Excitation mechanisms and discharge characteristics-recent developments. In *Inductively Coupled Plasma Emission Spectroscopy, Part 2*; Boumans, P.W.J.M., Ed.; John Wily & Sons: New York, 1987; 387–420.
25. Duffendach, O.S.; Black, J.G. Studies on the spctra of Cu I, Cu II, and Mn II by means of a vacuum tungsten furnace. Phys. Rev. **1929**, *34*, 35–43.
26. Goldwasser, A.; Mermet, J.M. Contribution of the charge-transfer process to the excitation mechanisms in inductively coupled plasma atomic emission spectroscopy. Spectrochim. Acta **1986**, *41B*, 439–725.
27. Wagatsuma, K.; Danzaki, Y. Non-Boltzmann distribution among energy levels of singly-ionized vanadium in DC glow discharge and RF inductively coupled discharge plasmas. J. Anal. At. Spectrom. **1999**, *14*, 1727–1730.

Received September 30, 2002
Accepted February 18, 2003

MARCEL DEKKER, INC.
270 Madison Avenue, New York, New York 10016